Use of Conformal Mapping in Grid Generation for Complex Three-Dimensional Configurations

N. D. Halsey*
Douglas Aircraft Company, Long Beach, California

Conformal mapping is a very useful but underexploited tool in the construction of body-fitted finite-difference (or finite-volume) grids for complex three-dimensional configurations. It has been used frequently for many two-dimensional problems and, to a lesser extent, for simple three-dimensional configurations such as isolated wings or nacelles and wing/body combinations. This paper describes applications of conformal mapping in generating grids about three-dimensional nacelles with and without other aircraft components in close proximity. In the most complicated case considered, a grid is generated about an aft-fuselage-mounted nacelle/pylon configuration.

Introduction

In recent years there has been a dramatic increase in the ability to compute transonic flow over three-dimensional configurations. The complexity of the field equations being considered has steadily increased from the small disturbance potential methods of Boppe[1] to the full-potential methods of Jameson[2] and more recently even to Euler and Navier-Stokes methods. The complexity of the geometry being considered has also increased from the isolated wings of Jameson[2] or the isolated nacelles of Arlinger[3] to the simplified wing-fuselage representations of Caughey and Jameson,[4] the improved wing-fuselage combinations of Chen,[5] the wing-body-tail geometries of Shmilovich,[6] and the more nearly complete aircraft geometries of Lee.[7] Because of the great generality of the finite-volume flow solution methods,[8] it can be argued that the main difficulty in analyzing more complex configurations concerns the grid-generation.

A variety of methods are commonly employed in grid generation, ranging from very simple algebraic methods to quite elaborate elliptic-equations methods. Each method, properly implemented, can produce effective grids for certain configurations, but by no means is there any universal method that applies to all geometries. In fact, it is common for two or more techniques to be used together in a single problem. Conformal mapping can often be used to simplify the geometry and allow better grids to be generated with less computational effort. Its usefulness for two-dimensional geometries is well known. Several popular methods for single-element airfoils in transonic flow use conformal mapping. For example, the method of Bauer et al.,[9] which has been something of a standard code in the aircraft industry for the past ten years, makes use of a mapping to the interior of the unit circle. An alternative approach developed by Caughey[10] employs a conformal unwrapping of the airfoil about a point just inside its leading edge. Conformal mapping has also been used for grid generation about multielement airfoils,[11,12] axisymmetric nacelles,[3,13-15] irregular channels,[16] and other two-dimensional configurations.

Conformal mapping has also been used as an aid in the grid generation about certain three-dimensional configurations, but its use here has been much more limited. Notable examples include (among others) the wing-alone method of Jameson,[2] the wing-body methods of Caughey and Jameson[4] and of Chen[17] and Chen et al.,[18] and the isolated nacelle methods of Ives and Menor.[13]

It is the author's opinion that much more extensive use could be made of conformal mapping in the grid generation about complicated three-dimensional configurations. This paper describes the application of conformal mapping to several grid-generation problems involving three-dimensional nacelles. The cases considered progress in complexity from an isolated nacelle, a nacelle near a reflection plane, a nacelle near a fuselage, a nacelle and pylon near a reflection plane, finally to a nacelle and pylon mounted on the after portion of an aircraft fuselage. Since the methods are still under development, better grids will undoubtedly be obtained in the future. In particular, the algebraic functions used for distributing grid points in the transformed space are very elementary. However, the quality of the grids obtained so far definitely establish the feasibility of the basic approach. For clarity of presentation, the grids shown in this paper are somewhat coarser than those actually used in flow calculations.

Isolated Three-Dimensional Nacelle

Grid generation about isolated three-dimensional nacelles requires only a very simple extension of the methods used for isolated axisymmetric nacelles. Such methods have been developed by Ives and Menor[13] and by Inoue.[15] Two-dimensional grids are generated on a sequence of planes passing through the nacelle center-line with a smoothly varying circumferential angle (usually with equal increments in the angle). Calculations on each plane are nearly independent of calculations on all other planes, except that the point spacing on the boundaries must vary smoothly from one plane to the next and the portions of the boundaries along the nacelle centerline must all have the same point spacing.

The discussion in this section will concentrate on the two-dimensional method for grid generation in each of the planes, which is really the heart of the three-dimensional method. The method described differs only in details from previous methods,[3,13-15] and no particular advantage to the current methods if claimed. It is included in order to introduce some of the mappings and to provide a foundation for the buildup of the more complex geometries described in later sections.

In any of the two-dimensional planes, the geometry under consideration has the general form shown in the first part of Fig. 1. The inner boundary consists of the nacelle cross section (A-B-C) and its horizontal extension downstream (C-D). The outer boundary consists of three straight line segments. Segment E-F coincides with the nacelle centerline, segment F-G falls on the upstream boundary, and segment G-H lies on the farfield boundary. The division of the outer boundary into

Presented as Paper 86-0497 at the AIAA 24th Aerospace Sciences Meeting, Reno, NV, Jan. 6-9, 1986; received Jan. 16, 1986; revision received Jan. 20, 1987.

*Senior Engineer/Scientist, Research and Technology Group, Aircraft Configuration and Performance. Member AIAA.

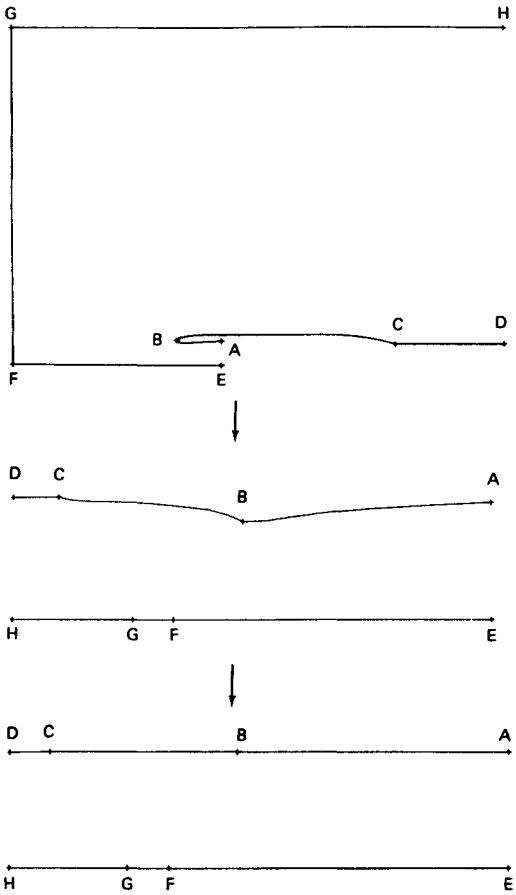

Fig. 1 Sequence of mappings for the nacelle.

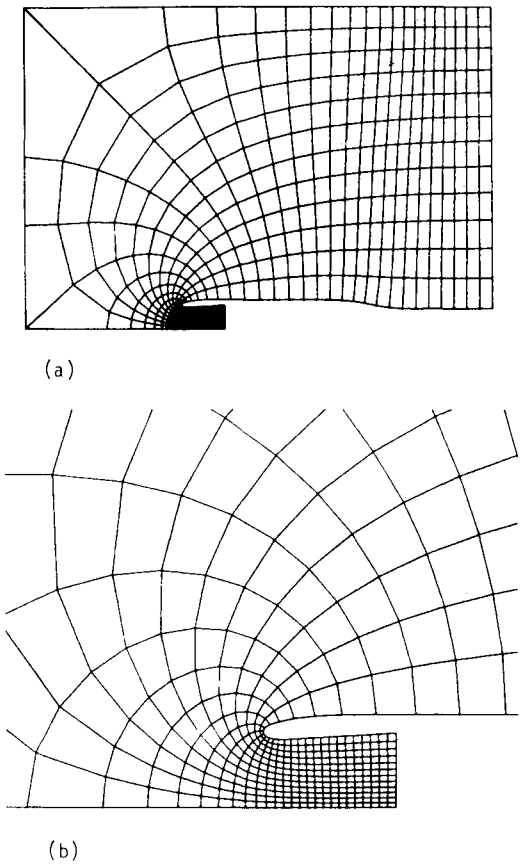

Fig. 2 Grid about an isolated nacelle.

three segments was dictated by requirements involving the more complicated geometries to be described later.

The first stage in the grid generation is to apply conformal mappings that transform the region between the inner and outer boundaries in the physical plane to the region between parallel boundaries. This is accomplished by a two-step process illustrated in Fig. 1.

The first step of this transformation is an analytic unwrapping of the nacelle profile about a singular point near the center or curvature of its leading edge. In the process, the outer boundary of the region is transformed to a horizontal line above the image of the nacelle profile. This is accomplished using the mapping function

$$Z_2 = a + (1-b)L_1 + bL_2 \tag{1}$$

where

$$L_1 = 2\ell n\,(f_1 + f_2) \tag{2}$$

$$L_2 = 2\ell n(\sqrt{-d}f_1 + \sqrt{-c}f_2) - z_1 \tag{3}$$

$$f_1 = (e^{Z_1} - c)^{1/2} \tag{4}$$

$$f_2 = (e^{Z_1} - d)^{1/2} \tag{5}$$

In these equations, Z_1 and Z_2 are the complex coordinates before and after the transformation, a and b are complex constants, and c and d are real constants determined from the geometry in the Z_1 plane. This mapping was derived by combining a Schwarz-Christoffel mapping with a mapping between the upper half-plane and a parallel channel. For the special case in which the nacelle cross section is a flat plate, the region is transformed to the rectangular region between parallel walls without the need for the further step described next.

The second step of this sequence transforms the curve A-B-C-D to a horizontal line while preserving the horizontal boundary E-F-G-H. After an initial rotation and translation of coordinates to position E-F-G-H on the real axis, this is accomplished using the mapping function

$$Z_2 = Z_3 + \sum_{j=0}^{\infty} [\,(a_j + ib_j)e^{+ijZ_3} + (a_j - ib_j)e^{-ijZ_3}\,] \tag{6}$$

where Z_3 is the complex coordinate after the transformation and a_j and b_j are coefficients of an infinite series. A finite number of these coefficients are computed using fast Fourier transforms and a rapidly converging iteration procedure. This procedure is an adaptation of a method originally developed by Garrick[19] and more recently implemented using modern numerical techniques by Ives.[20]

Once the transformations have been performed, simple algebraic techniques in the transformed plane are used to distribute points on the boundaries and in the area between them. Finally, the mappings are performed in reverse order to map each grid point back to the physical plane. In the simplest case, a uniform rectangular grid in the transformed plane can be used. This is usually not satisfactory however, because a grid point does not necessarily coincide with each of the corner points on the outer boundary and because the relative sizes of the cells inside and outside the inlet are uncontrolled. In the current method, the number of points on each segment of the inner and outer boundaries is specified, and simple stretching functions are used to distribute points smoothly in between. Grid points in the interior of the region are found by computing the intersections of straight lines parallel to the boundaries and cubic curves connecting corresponding points on the boundaries. Figure 2 shows an example of a grid constructed by this procedure.

Three-Dimensional Nacelle Near a Plane of Symmetry

The next step in increasing complexity of the geometry is to consider a three-dimensional nacelle near a reflection plane parallel to the nacelle centerline. The desired grid is very

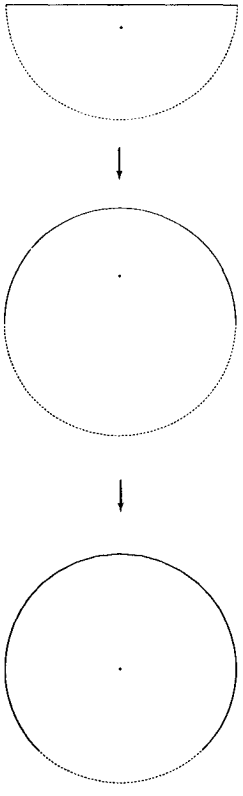

Fig. 3 Sequence of mappings for the symmetry plane.

similar to the grid for an isolated three-dimensional nacelle, except that the outer boundary surface now consists of two segments—one flat and one semicylindrical. The entire grid will thus be contained within half of a right circular cylinder. The general strategy for the grid generation in this case is to use conformal mapping to transform the half-cylinder to a full cylinder with the nacelle centerline on the cylinder's axis, generate the grid within the cylinder using the previously described method for isolated three-dimensional nacelles, and then perform the new mappings in reverse to get the points back to physical space.

The half-cylinder is transformed to a full cylinder by a mapping in planes perpendicular to the axis of the half-cylinder. Since the cylinder and half-cylinder have constant radii, a single mapping (independent of axial location) is sufficient. The function to accomplish this mapping is

$$Z_2 = \frac{-(1-iZ_1)^2 + i(1+iZ_1)^2}{(1+iZ_1)^2 + i(1-iZ_1)^2} \tag{7}$$

where Z_1 and Z_2 are the complex coordinates before and after the transormation respectively. This function was derived by combining the known transformations[21] between a semicircle and the upper half-plane and between the upper half-plane and a circle.

A second mapping moves the image of the nacelle centerline to the axis of the cylinder while preserving the cylinder. The function to do this is a linear fractional transformation

$$Z_3 = \frac{(Z_2 - \alpha)}{(1 - \bar{\alpha} Z_2)} \tag{8}$$

where Z_3 is the complex coordinate after the transformation and α is a complex constant equal to the coordinate of the nacelle centerline in the Z_2 plane. Assuming the nacelle centerline to be straight, this mapping is also independent of axial location in the cylinder. The two mappings of this sequence are illustrated in Fig. 3.

The mappings to transform the outer boundary to the surface of the cylinder must also be applied to the points defining

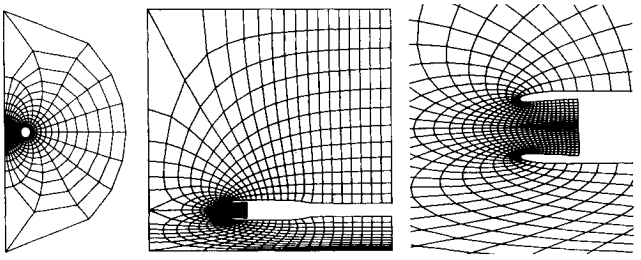

a) b) c)

Fig. 4 Grid about a nacelle near a symmetry plane.

the nacelle. Even if the nacelle were initially axisymmetric, the slight distortion due to these mappings makes the nacelle fully three-dimensional at this point in the calculations.

The construction of the grid within the cylinder in the transformed space is nearly identical to the method described in the previous section. In this case, however, it is desired to force a grid line to lie along each of the two intersections between the plane of symmetry and the half-cylinder (in the physical space). This can be done by applying a stretching function to define the curve of angular coordinate vs point number in the transformed space. Alternatively, the radius of the original half-cylinder can be specified in such a way that a grid line falls along each intersection curve when equally spaced planes are used.

Figure 4 shows a typical grid generated using this method. Figure 4a shows a cross section of the grid in the plane perpendicular to the axis of the cylinder. This illustrates the method's tendency to cluster the grid points in the area between the nacelle and the plane of symmetry, to spread them out elsewhere, and to produce curved surfaces that are nearly normal to the outer boundary and the nacelle surface. These features would be very difficult to produce with a purely algebraic method and relatively expensive with a differential equation method, but they occur naturally with a conformal mapping method. If necessary, simple functions can be used to cluster grid points more densely near the corners between the symmetry plane and the far-field boundary. Figures 4b and 4c show a cross section of the grid in the plane containing the nacelle centerline and perpendicular to the plane of symmetry. These illustrate one of the compromises that is inevitable with this configuration and all of those in the later sections: the number of grid points on each segment of the outer boundary must be the same on the left and right halves of the configuration, in spite of the radically different proportions of the halves. In spite of this, the grids produced by this method are very smooth, with tolerable skewness and distortion, and should allow the accurate calculation of the flowfield to be performed.

Three-Dimensional Nacelle/Fuselage Combination

The grid-generation method for a nacelle/fuselage combination is very similar to that for the nacelle and plane of symmetry already described. Consider first the simplest case: a three-dimensional nacelle near a cylindrical fuselage with the nacelle centerline parallel to the fuselage axis. In this case, applying the well-know Joukowski transformation maps the fuselage surface onto a portion of the plane of symmetry, reducing the geometry to that considered in the previous section. A slightly different stretching function must be used to ensure that grid lines coincide with the line of intersection between the fuselage and plane of symmetry as well as between the far-field boundary and the plane of symmetry.

In more general cases, with noncylindrical fuselage and possibly an angled or curved nacelle centerline, further changes are needed. The simple Joukowski is replaced by a two-step mapping sequence to transform the fuselage to the plane of symmetry, and the mapping parameters are functions that vary along the axis of the configuration.

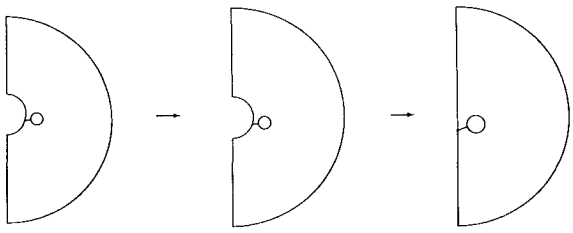

Fig. 5 Sequence of mappings for the fuselage.

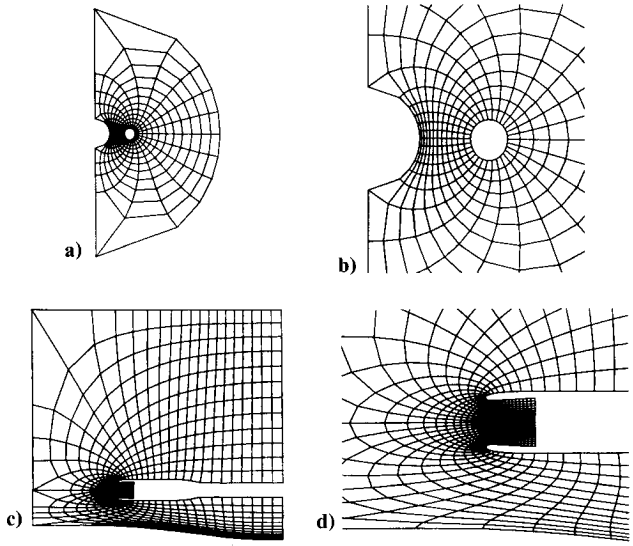

Fig. 6 Grid about a nacelle/fuselage combination.

The first mapping of the two-step sequence transforms the fuselage cross section to a circle while preserving the circular shape of the outer boundary of the grid. This is accomplished using the mapping function

$$Z_1 = Z_2 e^B \tag{9}$$

where

$$B = \sum_{j=0}^{\infty} [(-a_j + ib_j)\ (\hat{r}z_2)^j + (a_j + ib_j)\ (\hat{r}/Z_2)^j] \tag{10}$$

In these equations, Z_1 and Z_2 are the complex coordinates before and after the transformation, respectively; a_j and b_j are coefficients of an infinite series; and $\hat{r}$ is the radius of the circle to which the fuselage cross-section maps (normalized by the radius of the outer circle). This function is very similar to the function Eq. (6). More details of the derivation and use of this mapping have been given by Ives.[20]

The second mapping of this sequence transforms the circular fuselage cross section to a flat plate conciding with the spanwise plane of symmetry while preserving the circular shape of the outer boundary. This is accomplished using the function

$$Z_3 = Z_2 \left(\frac{1-\hat{r}^2 Z_2^{-2}}{1-\hat{r}^2 Z_2^{+2}}\right)\left(\frac{1-\hat{r}^6 Z_2^{+2}}{1-\hat{r}^6 Z_2^{-2}}\right)\cdots \tag{11}$$

where Z_3 is the complex coordinate after the transformation. This function is a special case of a transformation explained in Nehari,[21] and was derived using an infinite product expansion for the Jacobi elliptic function $[SN(Z_2,\hat{r})]$. For typical values of $\hat{r}$, the infinite product converges extremely rapidly; usually only about three terms are needed to compute the function to machine accuracy. For sufficiently small values of $\hat{r}$, the function approaches the more familiar Joukowski transformation.

With the addition of these two mappings, the sequence of mappings in planes perpendicular to the fuselage axis now consists of four mappings. Although some authors have been critical of mapping methods requiring multiple steps,[15] many transformations can be derived and implemented more quickly and computed more efficiently and accurately using a sequence of mappings. In the present case, only the first step requires the numerical determination of mapping parameters, and these are found very easily using fast Fourier transforms. The three remaining steps use purely analytic mappings. To accomplish the same transformation in a single step would not be desirable, since a much larger portion of the total mapping would be determined by numerical means of more limited accuracy. The mapping sequence for the fuselage is illustrated in Fig. 5.

For a general configuration, most of these mappings must be computed as functions of axial location. If the shape of the fuselage cross section varies along the axis, the coefficients of the series expansions in the first mapping also vary along the axis. If the radius of the fuselage after the first mapping varies along the axis, then the term $\hat{r}$ in the second mapping also varies. The third mapping is the same for all axial locations. If the nacelle centerline is not straight and parallel to the fuselage axis at the start of the calculation, or if the first two mappings distort it, then the constant in the fourth mapping also varies along the axis. Transformations must be applied at general points on the nacelle and fuselage that do not necessarily lie in planes on which the mapping parameters have been computed. Interpolation of the mapping parameters is therefore required. For cases considered to date, third-order Lagrangian interpolation using ten to twenty stations along the fuselage axis has been found to be adequate.

At this stage in the calculations, the region in which the grid is to be constructed has been mapped to the interior of a circular cylinder with the nacelle centerline along the cylinder's axis. Thus, the transformed space is the same as in the case of the nacelle near a plane of symmetry or the nacelle near a cylindrical fuselage. However, in this case, the crown lines representing the intersection curves of the fuselage and far-field boundary with the plane of symmetry are no longer straight nor parallel to the axis of the cylinder. In the current method, nonconformal shearings are applied to straighten them. These shearings are derived section by section along the axis. At each section, functions are defined that have maximum influence on the circumference, reduce smoothly to zero at the axis, and move the four intersection points to specified locations.

The remainder of the grid-generation procedure is the same as in the simpler case with the cylindrical fuselage. Figure 6 shows a grid generated using this method.

Three Dimensional Nacelle/Pylon Combination with a Plane of Symmetry

The methods for the two previous configurations each made use of two sets of conformal mappings, the first set working in planes normal to the fuselage and/or nacelle axis and the second set working in planes at right angles to these. The first set of mappings transformed the three-dimensional region under consideration to the interior of a circular cylinder. However, no particular significance was attached to the three-dimensional geometry resulting from the second set of mappings. In the current cases with three components, three sets of mappings will be used, and the three-dimensional significance of each set of mappings must be realized.

The first two sets of mappings are nearly identical to those described earlier for the case without the pylon, the main difference being the need to apply the mappings to the defining points on the pylon as well as to those on the nacelle and plane of symmetry. In each of the mappings of the second set, the region maps to the area between two parallel lines. The distance between the parallel lines varies slightly from one

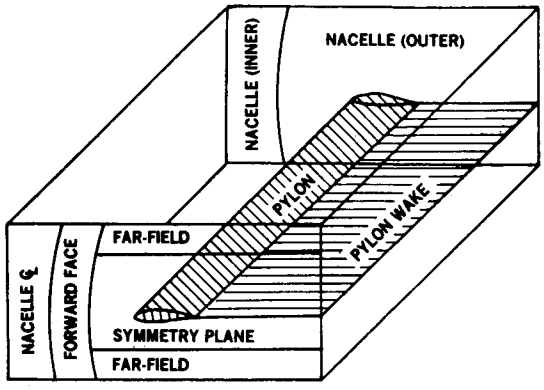

Fig. 7 Configuration after the second mapping sequence (schematic).

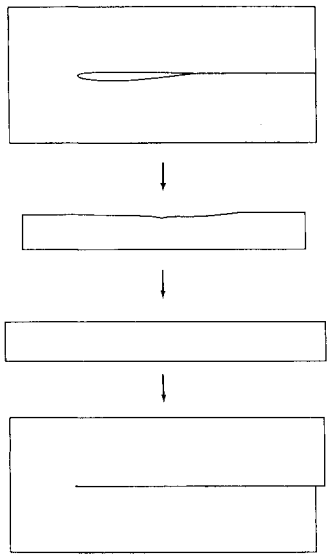

Fig. 8 Sequence of mappings for the pylon.

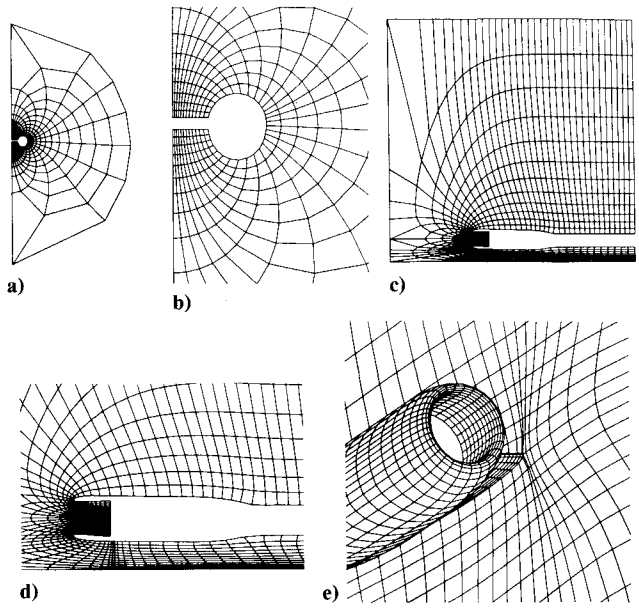

Fig. 9 Grid about a nacelle/pylon combination with a plane of symmetry.

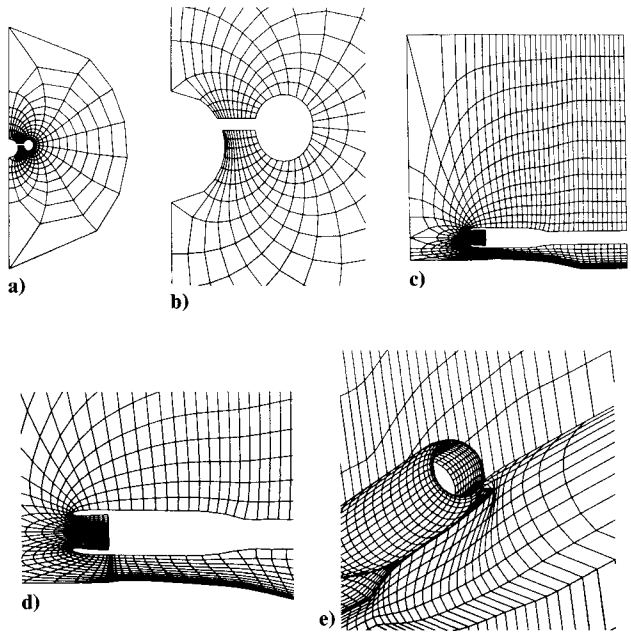

Fig. 10 Grid about an aft-fuselage-mounted nacelle/pylon combination.

mapping to the next, but this variation is eliminated by a small nonconformal scaling of the coordinates. Because of an arbitrary constant of translation that can be applied to each of the parallel lines, however, the three-dimensional significance of this set of mappings remains ambiguous. If zero translation were to be applied, the transformed geometry could be considered to be another cylinder with a slit along its axis. Assuming nonzero translation, the geometry becomes an "annular cylinder," a cylindrical region with the central area excluded. The pylon spans the distance between the inner and outer walls of this cylinder.

In order to construct a grid within this cylindrical region with the pylon, it is convenient to apply more transformations. A circumferential unwrapping of the configuration (using a simple logarithmic mapping function) reduces the region under consideration to a rectangular solid with the pylon spanning the distance between parallel faces. The radial planes on which the second set of transformations were performed transform to horizontal planes parallel to the span of the pylon. A sketch of the configuration at this stage of the transformations is shown in Fig. 7.

Over most of the configuration, a suitable grid can now be constructed easily without any further transformations. For each of the planes farther from the pylon than the planes containing the crown lines, an algebraic procedure is directly applied. This procedure is identical to the one described in the previous section.

Over the remainder of the configuration, grids are constructed in a succession of planes perpendicular to the span of the pylon. These grids are generated with the aid of a further conformal mapping to transform the pylon cross-section and its downstream extension to a flat plate. This mapping is accomplished in three steps. The first two steps are identical to the two steps of the mapping for the isolated nacelle. An analytical unwrapping about a singular point near the leading edge [using Eqs. (1-5)], followed by a numerical mapping to straighten the resulting curve [using Eq. (6)] results in a rectangular region. An application of the same analytical unwrapping in reverse, this time using a singular point on the line to which the pylon has been mapped, completes the desired transformation. The steps of this transformation are illustrated in Fig. 8.

The construction of the grid in this final transformed plane can be accomplished very effectively using simple algebraic techniques. Points on the upper and lower boundaries are chosen in order to match the portion of the grid already generated. Points on the pylon are chosen in such a way as to give a modified-cosine spacing after transforming back to the

stage shown in Fig. 7. Interior points are chosen to blend smoothly within these constraints.

The final step of the grid-generation procedure is to apply the transformations in reverse order to all the grid points. Applying the pylon mappings requires no interpolation of the mapping parameters, since all grids are constructed directly in the same planes in which these parameters are computed. Applying the nacelle mappings does require interpolation in the region in which the pylon mappings are used. Applying the fuselage mappings requires interpolation for all points. Figure 9 shows a grid for a nacelle/pylon combination near a plane of symmetry, constructed using the method described above.

Three Dimensional Aft-Fuselage-Mounted Nacelle/Pylon Combination

The most complex geometry considered in this paper is a nacelle/pylon combination mounted on the after portion of an aircraft fuselage. The method for generating the grid about this configuration combines the methods described for the previous two configurations. Applying the mapping sequence of Fig. 5 reduces the geometry to a nacelle/pylon combination with a reflection plane. The grid about this configuration is constructed as described in the previous section, with only minor modifications needed to conform grid lines to the lines of intersection of the fuselage and the symmetry plane.

Figure 10 shows a grid for this configuration. This grid would have been very difficult to generate using purely algebraic or differential-equation methods.

Conclusion

Workers in the area of computational fluid dynamics have used a wide variety of techniques to help them generate suitable grids. Conformal mapping is one of those techniques which has proven to be extremely valuable in the grid generation for two-dimensional and relatively simple three-dimensional configurations. It can also be extremely valuable for the most complex three-dimensional configurations. This paper has illustrated its usefulness for a variety of geometries involving nacelles and other aircraft components, the most complex case considered being an aft-fuselage-mounted nacelle/pylon combination. Further applications of conformal mapping could be of similar value in generating grids for wing-mounted nacelles, multielement wings, horizontal and vertical stabilizers, and other aircraft components. Grid generation about complete aircraft configurations is such a formidable problem that investigators working in that area cannot afford to neglect such a valuable tool.

Acknowledgment

The work reported in this paper was conducted under the sponsorship of the Independent Research and Development Program of the McDonnell Douglas Corporation.

References

[1]Boppe, C.W. "Computational Transonic Flow about Realistic Aircraft Configurations," AIAA Paper 78-104, Jan 1978.

[2]Jameson, A. "Iterative Solution of Transonic Flows over Airfoils and Wings, Including Flows at Mach 1" *Communications on Pure and Applied Mathamatics,* Vol. 27, May 1974, pp. 283–309.

[3]Arlinger, B.G., "Calculations of Transonic Flow Around Axisymmetric Inlets." *AIAA Journal*, Vol. 13, Dec. 1975, pp 1614–1621.

[4]Caughey, D.A. and Jameson, A. "Numerical Calculation of Transonic Potential Flow about Wing-Body Combinations," *AIAA Journal,* Vol. 17, Feb. 1979, pp. 175–181.

[5]Chen, L.T., Caughey, D.A., and Verhoff, A, "A Nearly Conformal Grid-Generation Method for Transonic Wing-Body Flowfield Calculations," AIAA Paper 82-108, Jan. 1982.

[6]Shmilovich, A. and Caughey, D.A., "Grid Generation for Wing-Tail-Fuselage Configurations," *Advances in Grid Generation*, edited by K.N. Ghia and U. Ghia, American Society of Mechanical Engineers, 1983, pp. 189–197.

[7]Lee, K.D., Huang, M., Yu, N.J., and Rubbert, P.E., "Grid Generation for General Three-Dimensional Configurations," *Numerical Grid Generation Techniques*, NASA Conf. Pub. 2166, Oct. 1980. pp.335–66.

[8]Jameson, A. and Caughey, D.A., "A Finite Volume Method for Transonic Potential Flow Calculations," AIAA Paper 77-635, June 1977.

[9]Bauer, F., Garabedian, P., Korn, D. and Jameson, A. "Supercritical Wing Sections," *Lecture Notes in Economics and Mathematical Systems,* Vol. 66, Springer-Verlag, New York, 1972.

[10]Caughey, D.A. "A Systematic Procedure for Generating Useful Conformal Mappings," *International Journal for Numerical Methods in Engineering* , Vol. 12, Nov. 1978, pp. 1651–1657.

[11]Halsey, N.D., "Conformal Grid Generation for Multielement Airfoils," *Numerical Grid Generation,* edited by J.F. Thompson, North Holland, New York, 1982, pp. 585–600.

[12]Halsey, N.D., "Calculation of Compressible Potential Flow About Multielement Airfoils Using a Source Field-Panel Approach," AIAA Paper 85-0038, 1985.

[13]Ives, D.C. and Menor, W.A. "Grid Generation for Inlet and Inlet-Centerbody Configurations Using Conformal Mapping and Stretching," AIAA Paper 81-0997, 1981.

[14]Chen, L.T. and Caughey, D.A. "Higher-Order Finite-Difference Scheme for Three-Dimensional Transonic Flowfields about Axisymmetric Bodies," *Journal of Aircraft,* Vol. 17, Sept. 1980, pp.668–676.

[15]Inoue, K. "Grid Generation for Inlet Configurations Using Conformal Mapping," *Journal of Computational Physics,* Vol. 58, March 1985, pp. 146–154.

[16]Floryan, J.M. "Conformal-Mapping-Based Coordinate Generation Method for Flows in Periodic Configurations," *Journal of Computational Physics*, Vol. 62, Jan. 1986, pp. 221–247.

[17]Chen, L.T. "A More Accurate Transonic Computational Method for Wing-Body Configurations," *AIAA Journal,* Vol. 21, June 1983, pp. 848–855.

[18]Chen, L.T., Vassberg, J.C., and Peavey, C. C. "A Transonic Wing-Body Flowfield Calculation with Improved Grid Topology and Shock-Point Operators," AIAA Paper 84-2157, Aug 1984.

[19]Garrick, I.E., "Potential Flow About Arbitrary Biplane Wing Section," NACA Rept. 542, 1936.

[20]Ives, D.C., "A Modern Look at Conformal Mapping Including Multiply Connected Regions," *AIAA Journal,* Vol. 14, Aug. 1976, 1006–1011.

[21]Nehari, Z. *Conformal Mapping,* McGraw-Hill, New York, 1952.